CFD Letters 16, Issue 7 (2024) 71-88

SEMARAK ILMU PUBLISHING

CFD Letters

Journal homepage:
https://semarakilmu.com.my/journals/index.php/CFD_Letters/index
ISSN: 2180-1363

Comparison of 2D and 3D Simulations on Predicting the Performance of a Savonius Wind Turbine

Ahmad Adib Najib[1], Djamal Hissein Didane[2,*] Mostafa Radwan Behery[1], Hashim Ahmed Kabrein[3]

[1] Faculty of Mechanical and Manufacturing Engineering, University Tun Hussein Onn Malaysia, 86400 Parit Raja, Batu Pahat, Johor, Malaysia
[2] Center for Energy and Industrial Environment Studies (CEIES), Faculty of Mechanical and Manufacturing Engineering, Universiti Tun Hussein Onn Malaysia, Malaysia
[3] Faculty of Engineering, International University of Africa, Sudan

ARTICLE INFO

Article history:
Received 27 September 2023
Received in revised form 21 October 2023
Accepted 20 November 2023
Available online 29 February 2024

Keywords:
Savonius rotor; Wind energy; Performance analysis; 2D and 3D analysis; Renewable energy

ABSTRACT

The performance of Savonius rotors plays a vital role in harnessing wind energy for various applications. This study aims to investigate and compare the performance characteristics of Savonius rotors using two-dimensional (2D) and three-dimensional (3D) analysis approaches. The primary objective is to determine the optimal analysis method for evaluating the rotor's performance. The simulations were conducted using ANSYS software, considering six different tip-speed ratios (TSRs) ranging from 0.2 to 1.2, and three wind speed categories (7 m/s, 5 m/s, and 3 m/s). The hybrid shear-stress transport (SST) k-omega was used as the turbulence model. The results indicate that the 2D analysis approach, which simplifies the rotor's geometry by assuming rotational symmetry, provides reasonable estimations of the rotor's performance. However, the 3D analysis captures the intricacies of the rotor's actual geometry, accounting for the effects of non-uniform flow and vortex shedding, which can significantly influence the rotor's performance. The comparative analysis reveals that the 3D analysis predicts higher torque and power coefficients than the 2D approach, especially at higher wind speeds. At TSR 1.0, the torque and power coefficient obtained from the 3D approach are 6.56 Nm and 0.102, respectively meanwhile 2D approach gains 6.28 Nm torque and 0.098 for power coefficient. This research contributes to a better understanding of the performance characteristics of Savonius rotors and highlights the importance of considering three-dimensional effects in their analysis. The findings can guide the design and optimization of Savonius rotor systems, leading to improved wind energy conversion efficiency and enhanced utilization of renewable energy resources.

1. Introduction

Energy is crucial for economic growth and our overall well-being. However, overreliance on non-renewable energy sources can lead to irreversible problems [1, 2]. The biocapacity of our planet is being overused, and our ecological footprint exceeds the earth's regeneration capabilities. This means that non-renewable energy may not be available in the future [3, 4]. Moreover, a great number of studies in recent years have shown that the amount of energy consumed by the earth's

* *Corresponding author.*
E-mail address: djamal@uthm.edu.my (Djamal Hissein Didane)

https://doi.org/10.37934/cfdl.17.6.7188

population is increasing yearly. Excessive use of dirty energy (non-renewable) sources is constantly rising in a diverse range of economic areas which, in turn, exacerbates global warming and other environmental issues [5]. Due to these problems, research on renewable energy is being conducted widely all around the world. This kind of energy can be said almost non-pollutive to the environment. A variety of renewable resources can be used to produce energy [6]. According to Aktaş [7], the sun provides us with solar energy and to properly extract solar energy, different types of technologies must be used, the easiest example is the solar panel. Many kinds of technologies can be used to produce energy from the sun [8]. The same goes for the other types of renewable resources. Almost all of them can be used to produce energy. Water or more specifically wave energy is also one of the resources that can be said to be almost inextinguishable on Earth as the seas cover almost two-thirds of the earth's surface. Wave energy is a renewable source of power with enormous potential that seems to be underexploited [9]. Other resources such as geothermal and biogas are also good energy resources, however, if these energies are not properly managed, they might cause some environmental problems despite being considered a clean source of energy, even wind energy can be turned into electricity [10].

However, wind energy is among the fastest forms of renewable energy today. According to Al-Quraishi *et al.,* [2], wind energy is produced whenever the atmosphere is heated by a small amount of solar radiation. Because of its straightforward functionality, the wind is a sustainable energy source that is domestic, consistent, clean, does not harm the environment, and has no fuel/raw material cost. Moreover, the most recognized method used to harvest wind energy is by using the wind turbine [11]. The wind turbine itself does not contribute to any kind of pollution to the environment, they are not even making any greenhouse effect [12]. The addition of continuous studies and research is making wind turbines much more convenient day by day. Furthermore, the long lifespan of wind turbines makes them more reliable, even if the early investment is high, it is considered worth it as it will provide continuous energy [13]. There are typically two types of wind turbines. Horizontal axis wind turbines (HAWTs) and vertical axis wind turbines (VAWTs). The HWAT is widely used due to its better conversion efficiency compared to the VAWT. However, the latter also has started to gain attention in the recent years [14]. The development of technologies regarding wind energy harvesters has never stopped since researchers all around the world keep trying to find a way/method that can be used to improve the performance of wind turbines while keeping their advantages [15]. This magnificent development also led to studies regarding the Savonius rotor wind turbine, one of the well-known categories of VAWT alongside the Darrieus rotor. According to Dewan *et al.,* [16], compared to Darrieus rotors, Savonius rotors are better at starting and can work in low-wind conditions, besides being of low noise, easy installation, and straightforward design.

Savonius rotors operate as the flow of fluid pushes the advancing blade dragging it forward, hence rotating the blade and bringing the returning blade to the initial position of the advancing blade. The primary mechanism causing Savonius-type rotors to rotate is the drag force difference between the concave (advancing blade) and convex (returning blade) sides of the rotor blades [17, 18]. According to Didane *et al.,* [19], the concave side of the rotor experiences a greater drag force than the convex side when the incoming wind contacts it. Thus, the main driving component of the S-type rotors is based on drag force. Thus, the Savonius Rotor operates primarily as a result of wind drag forces acting on its buckets, but lifting forces also help transmit mechanical power to the shaft. The limitation is that the rotor's rotational speed cannot be greater than the speed of the wind results from the drag force-based operating principle [20]. This is the main cause of their TSR being limited to a gain of no more than 1 [21]. Thus, the negative torque is produced from the rotating Savonius rotor. This is one of the disadvantages of the Savonius rotor. However, Savonius turbines have a huge deficiency in the rate of energy conversion compared to other turbine rotors [22]. In addition, Al-Gburi *et al.,* [23] also stated that the returning blade of the Savonius rotor produces lots of negative torque.

The quest to improve the performance of the rotor is still underway as the conversion rate of this turbine is still considered unsatisfactory [24, 25]. Tian *et al.,* [26] performed an extensive study on the performance of the Savonius rotor and proposed four methods that can be used to improve the performance of the said turbine which are optimization of the basic parameters of the rotor, enhancing the wind blades in the aspect of geometric characteristics, adding support to the blades and Improving the flow field around the blade. Other than that, Yuwono *et al.,* [27] stated that Savonius wind turbine performance can be improved by positioning a cylinder in a circle in front of the returning blade (upstream). Similarly, Duc *et al.,* [28] studied the effect of a multicurve shape on the Savanious rotor and concluded that 20% performance improvement was obtained. In addition to that, Al-Ghriybah *et al.,* [29] proposed to adjust the rotor's configurations with an external overlap to further improve the performance of the rotor. Other researchers proposed the idea of adding a deflector to the Savonius rotor to enhance the intrinsic capacities of the rotor [30]. Apart from that the new counter-rotating technique is being used nowadays to improve the performance of VAWTs as it increases the conversion capabilities extensively [31–35]. Furthermore, the number of blades also affects the performance of the Savonius rotor [36]. A study conducted by Wenehenubun *et al.,* [37] concluded that the number of blades influences the rotation of the rotor of wind turbine models. Contrary to this, Thiyagaraj *et al.,* [38] however, highlighted that the two-blade Savonius turbine has shown better performance characteristics than the 3, 4, 5 and 6-blade Savonius turbines. The result of each research varies perhaps due to some other unsolvable variable. In comparison to wind turbines with two and four blades, three blades produce higher rotational speed and TSR. Compared to wind turbines with two or three blades, those with four blades have a higher torque [19]. In addition, while three-blade wind turbines perform best at higher TSRs, four-blade wind turbines perform well at lower TSRs.

There are a few researchers who are interested in findings the simulation method that can produce results with the highest accuracy, between 2D and 3D CFD simulation. Chemengich *et al.* [39] studied the effect of variations of gap flow guide geometry on the performance of Savonius using 2D and 3D models. They conclude that the results of 2D and 3D are almost the same in certain parameters and slightly different in some other cases. Contrary, Ferrari *et al.,* [40] stated the trends are not uniform for the four parameters measured but consistent with the assertion done by Chemengich *et al.,* [39] about 2D and 3D models. However, they agreed that 3D is more advantageous than 2D in some cases of studies due to the limitation of 2D CFD analysis. This statement was also supported by Larin *et al.,* [41], stating that the 3D phenomena, such as flow bypass around the sides of the turbine and tip vortices, are not captured in 2D flow simulations, highlighting the importance of 3D flow simulation. However, in a simulation to evaluate the performance of Savonius rotor by Howell *et al.,* [42], the 2D method shows a higher performance difference compared to 3D. It was later found that the cause for the differences is the presence of tip vortices in the 3D model which is not present in the 2D simulations.

Thus, in this study, the main purpose is to investigate the most efficient method between 2D and 3D simulation that can be used to predict the performance of a wind turbine, specifically the Savonius wind turbine using computational fluid dynamics (CFD) technique.

2. Theoretical Formulations

2.1 *Governing Equations*

In this study, the governing equations and turbulence equations are examined to comprehend the fluid flow behavior. There are three unique components that may be extracted from the Navier-Stokes equations. These components include the conservation of mass, the conservation of momentum, and the conservation of energy. With the assistance of these equations, one is able to achieve an understanding of the temporal and spatial dynamics of the velocity, pressure, and temperature of a fluid. However, in this study, it is highlighted that only two of the three equations will be used which are the mass conservation equation and momentum conservation equation, as shown in Eq. (1) and Eq. (2), respectively.

$$\frac{\partial \rho}{\partial t} + \nabla \cdot (\rho v) = 0 \tag{1}$$

$$\partial \frac{(\rho v)}{\partial t} + \nabla \cdot (\rho v v) = -\nabla p + \nabla \cdot \tau + \rho g \tag{2}$$

where;

ρ, fluid density, t is time, u is fluid velocity, p is fluid pressure, τ is viscous stress tensor and g is gravity.

2.2 Turbulence Model Equation

In CFD, the turbulence equation for a Savonius turbine is often derived from the Reynolds-averaged Navier-Stokes equations. In order to model the turbulent flow as a mean flow, the equations governing the conservation of mass, momentum, and energy in a fluid flow must be modified to account for turbulence. The application and needed precision will guide the selection of the turbulence model. Popular turbulence models for modeling Savonius turbine flows include the k-epsilon, k-omega, Reynolds stress, and large eddy simulation (LES) models.

The k-omega model was selected to represent turbulence in this particular investigation. The behavior of turbulent flow is characterized by the k-omega turbulence model, which uses two transport equations to do so. The first equation accounts for turbulent kinetic energy (k), while the second equation accounts for the specific dissipation rate of turbulent kinetic energy (G). The Reynolds-averaged Navier-Stokes (RANS) equations are used as a starting point for deriving the following equations. The equation for turbulent kinetic energy (k) and the equation for dissipation rate of kinetic energy (ω) are given, as shown in Eq. (3) and Eq. (4), respectively. In addition, ANSYS FLUENT software v.22 was used throughout the computational simulation in the present study.

$$\frac{d(\rho\, k)}{dt} + \frac{d}{dx_j}(\rho\, k\, u_j) = P_k - \omega \tag{3}$$

$$\frac{d(\rho\, \omega)}{dt} + \frac{d}{dx_j}(\rho\, \omega\, u_j) = P_\omega + G - D \tag{4}$$

2.3 Performance Parameters Formulation

In addition to the governing equation used for the CFD analysis, the theoretical formula for the required parameter is also needed in order to evaluate the performance of the simulation models. To complete this study, there are five highlighted parameters which are turbine torque Eq. (5), theoretical torque Eq. (6), torque coefficient Eq. (7), theoretical wind power Eq. (8), power coefficient Eq. (9) and lastly the TSR (TSR) Eq. (10).

$$T = P\omega \tag{5}$$

$$T = \frac{1}{2}(\rho A V^2 R) \tag{6}$$

$$C_t = \frac{T}{\frac{1}{2}(\rho A V^2 R)} \tag{7}$$

$$Pt = \frac{1}{2}\rho\, A\, V^3 \tag{8}$$

$$Cp = \frac{P}{\frac{1}{2}\,\rho\, A\, V^3} \tag{9}$$

$$\lambda = \frac{\omega R}{V} \tag{10}$$

3. Methodology

3.1 Model and Spatial Domain Description

The modeling software Solidwork version 2021 is used to design the model of the Savonius rotor that is used for the study. For both simulation methods, 2D and 3D, the same model is used to ensure that the final result is comparable, as shown in Table 1. The original design for Savonius is used as a reference to build this model. Figure 1 shows the simulation rotor as well as the computational domain in 2D while demonstrating their dimensional details. The domain was divided into two, the stationary domain and the rotating domain. The rotating domain was circular and an appropriate size of 1.5 times the rotor diameter was used to avoid the domain influence in the performance results [31]. The 2D domain dimensions were 36D x 24D (33.3m x 22.2m) with the rotor placed 10D (9.25m) from the inlet and midway between the top and bottom wall boundaries as shown in Figure 1. The 3D case assumed the same dimensions as 2D but with a height of 6D (5.55m).

Table 1
Range of the design parameters

Parameter	Detail (m)
Diameter of the rotor (D)	0.925
Diameter of the blade (d)	0.50
Endplate diameter (DO)	1.1D
Height of rotor (H)	1.00
Overlap ratio (s/d)	0.15

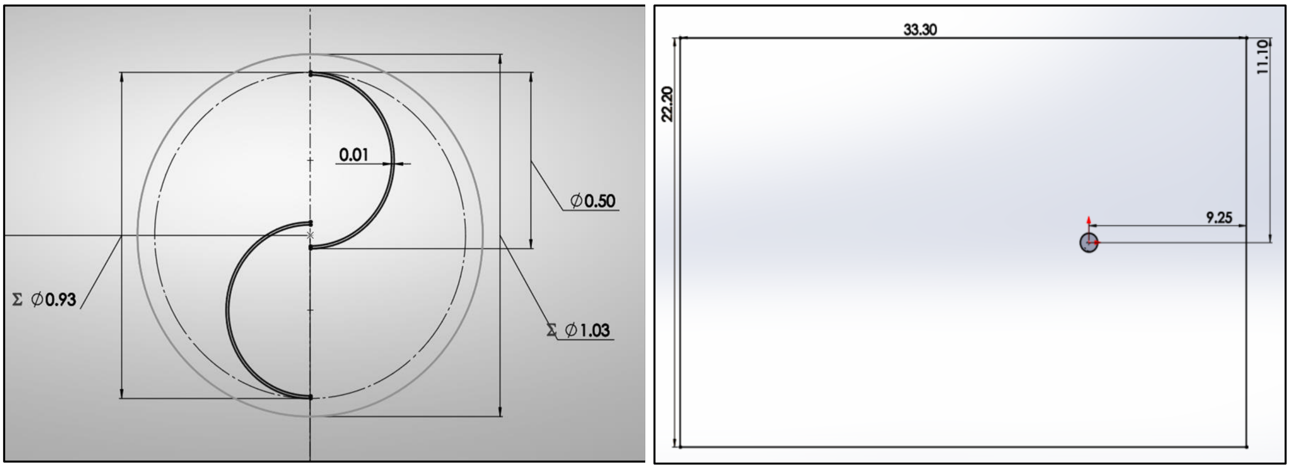

(a) (b)

Fig. 1. Simulation rotor and domain (a) Turbine rotor (b) Domain

3.2 Grid Generation and Simulation Setting

After a model has been created, the following step in pre-processing is to create the mesh also known as the grid. Grid generation or Mesh generation is the method used to divide the computational domain into a large number of smaller pieces, known as cells or elements. At this point, it's crucial to take extra precautions so that subsequent procedures go off without a hitch. When using the all-triangles approach, the sizing option allows the number of mesh cells to be changed based on the size of the pieces. The quality of the mesh cells formed in this procedure has a significant impact on the precision and accuracy of the resulting flow solution. The mesh cells employed in this analysis are clustered near the turbine blade. Inflation was applied to the area inside the domain's rotor, setting a maximum of 20 layers for the first layer. The first layer thickness is set to be 0.05 mm with a growth rate of 1.1. Next, adaptive sizing from the mesh sizing option was applied to obtain more homogeneous mesh cells throughout the domain, and we incorporate inflation to achieve the same goal towards the turbine edges, as shown in Figure 2.

In terms of boundary conditions, the inlet was assigned a condition of uniform and constant velocity of 7 m/s and the outlet a condition of uniform and constant atmospheric pressure. To avoid wall effects in the 2D case, the walls were chosen as symmetry. No-slip wall boundary conditions were imposed on the turbine blades as well as the interface between the edges of the rotating and stationary domains allowing flow properties to be transported [9]. The 3D case employed stationary, no-slip wall boundary conditions with the same inlet and outlet boundary conditions as the 2D case. The solver was configured as a pressure-based solver with an absolute velocity formulation and the simulations were solved using the SIMPLE algorithm and the SST k-omega turbulence model under time-dependant transient simulation. The SST, k-omega model was used due to its ability to accurately predict the pressure gradient and capture the swirling and rotating flows.

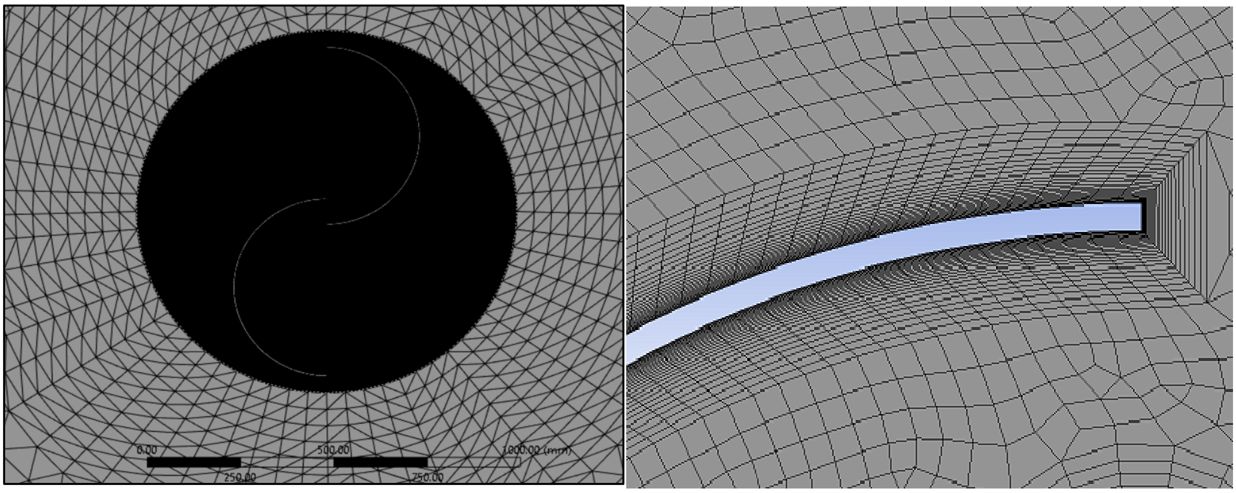

Fig. 2. 2D mesh of the model

4. Results and Discussion

4.1 Grid Independence Test

The mesh independence test was performed in the current study by evaluating the Torque of the rotor at TSR 0.6 for five different mesh densities of 147,000, 253,000, 489,000, 977,000, and 1,442,000 (very coarse, coarse, medium, fine, and very fine mesh) triangular cells in the 2D case. The simulation was allowed to run until the simulation result started to converge. The obtained data showed a very small difference between the medium and very fine mesh Torque values, as shown in Table 2. Therefore, to save on computational cost and time, the medium mesh was adopted to conduct the rest of the simulations, since it has been shown to predict the rotor performance with sufficient accuracy.

Table 2
Details of grid independence study for 2D

No	Size of Elements (mm)	No of Elements ($\times 10^6$)	Torque Output (Nm)	Percentage error (%)
1	8	0.147	4.2331672	9.66
2	4	0.253	5.0933672	8.69
3	2	0.489	4.8086296	2.62
4	1	0.977	4.4783355	4.43
5	0.5	1.422	4.7332163	1.01

4.2 Numerical Case Validation

To confirm the model's reliability, the current study was validated using the results from a previous study [39]. The geometrical details of the model used from the previous study and the current are identical with their details shown in Table 1. The numerical simulations were performed in identical conditions to the experimental tests. The Torque at TSR 0.2, 0.4, 0.6, 0.8, 1.0, and 1.2 for both simulations are compared with the experimental data. The average error for both simulations is calculated so that we can compare the differences between the simulation and experiment. From this validation, it can also be seen which simulation gives results closer to the actual experiment. Figure 3 shows the percentage error for both simulations. As shown from the figure, the average percentage error for 3D simulation is lower than for 2D simulation with 4.13% and 10.34% error, respectively.

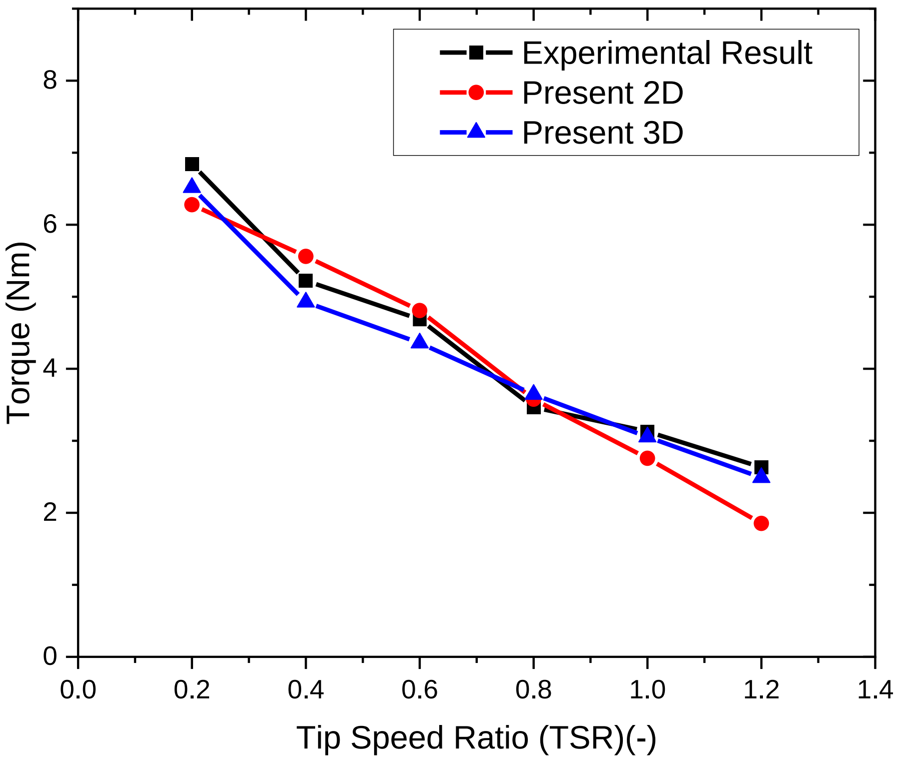

Fig. 3. Validation of torque output against TSR for 2D and 3D simulations

4.3 Comparison of Torque Output and Torque Coefficient

The comparison of torque and torque coefficient between 2D and 3D simulations is crucial in this study on the performance of Savonius rotors. The torque represents the rotational force generated by the rotor, while the torque coefficient allows us to compare the torque values across different rotor designs and operating conditions in a meaningful way. By comparing the torque and torque coefficient obtained from 2D and 3D simulations, we gain insights into the influence of three-dimensional effects on the rotor's performance. 2D simulations provide a simplified representation, assuming a two-dimensional flow and neglecting certain real-world effects such as end effects, tip clearance, and flow separation, which can significantly impact the generated torque. This comparison helps us assess how three-dimensional effects affect the torque output and consequently the power output of the rotor. It allows us to understand the limitations and advantages of 2D simulations as an approximation of real-world performance. Furthermore, the comparison of torque and torque coefficient guides us in making informed decisions about simulation approaches for future studies or design optimization. It helps us identify scenarios where 2D simulations may be sufficient and where 3D simulations are necessary for accurate predictions. The graph of torque against TSR and torque coefficient against TSR are plotted in Figure 4 and Figure 5, respectively.

The two figures display the relationship between the TSR and the corresponding torque values in the experimental result, 2D Simulation and 3D Simulations. Looking at the graph, it can be observed that as the TSR increases, the values of torque in all simulations tend to decrease. This suggests an inverse relationship between the TSR and the torque. It implies that as the TSR increases, the torque values measured during the simulation decrease. At the inlet velocity of 7 m/s, when the TSR is 0.2, we can see that the 2D model predicts a torque of 6.28 Nm, while the 3D model predicts a torque of 6.56 Nm. Both models underestimate the actual experimental result, indicating that they are not fully capturing the complexities of the system at this TSR. On the other hand, when the TSR is 1.2, the experimental result decreases to 2.63 Nm. In this case, the 2D model predicts a torque of 1.85 Nm, while the 3D model predicts a torque of 2.44 Nm. Again, both models underestimate the experimental result, however, the 3D model is closer to the actual value compared to the 2D model. These specific data points provide insights into the performance of the models at extreme TSR values. The underestimation of torque by both models at TSR 0.2 suggests that the models might not fully capture the fluid dynamics and interactions at low TSRs. Meanwhile, the discrepancy between the models and the experimental result at TSR 1.2 suggests that further improvements are needed to better account for the complex flow phenomena occurring at high TSRs.

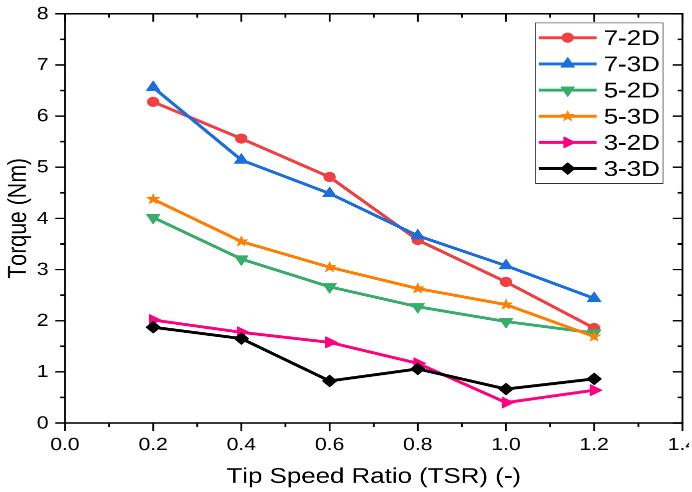

Fig. 4. Torque output against TSR at different wind speeds

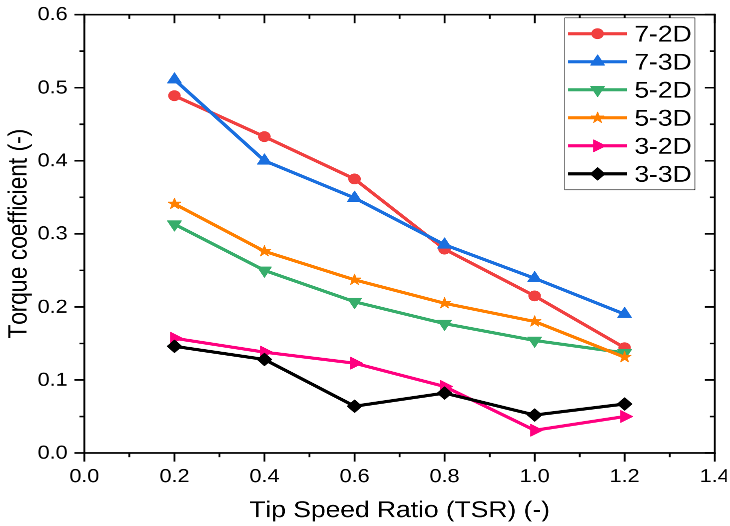

Fig. 5. Torque coefficient against TSR at different wind speeds

Moreover, the simulation is then expanded by changing one of the main parameters for the simulation, which is the wind velocity. Two other categories of simulation were simulated using wind speeds of 5 m/s and 3 m/s. From the graph, it can be observed that as the wind speed decreases, the torque predicted by the simulation also decreases. The specific trend of the data however is not the same for all three categories of simulation. This can be seen in the simulation graph for 5 m/s as there is a clear gap between the results of 2D and 3D simulations with 3D results being above 2D results at all TSR except at TSR 1.2. This is clearly different for the other 2 categories,7 m/s and 3 m/s where the plotted graph seems to be intertwined between 2D and 3D. From this, it can be said that the torque generated by the Savonius turbine is influenced by the wind speed. As the wind speed decreases, the available kinetic energy in the wind also decreases. This reduction in wind speed directly affects the amount of power that can be extracted from the wind, which subsequently impacts the torque generated by the wind turbine. When the wind speed decreases, there is less kinetic energy available in the wind, resulting in a lower force being exerted on the rotor blades. This reduced force translates to a decrease in torque. In simpler terms, the wind has less power to transfer to the blades, leading to a lower torque output. From the graph, it can also be observed that the relationship between wind speed and torque is not linear. In summary, the decrease in torque as wind speed decreases is due to the reduction in the available wind energy, resulting in a lower force being exerted on the rotor blades of the wind turbine. However, it can also be seen that even when the wind speed decreases, the simulation always predicts that the torque produced by 3D simulations is always above 2D simulations except for some point where it is slightly lower. It can be concluded that the models, particularly the 2D model, tend to underestimate the torque values compared to the experimental results across various TSRs. This highlights the limitations of the models in accurately predicting the behavior of the system. Further refinement of the models, potentially incorporating three-dimensional effects, is necessary to improve their accuracy and alignment with experimental findings. It is worth noting that the 3D model tends to provide slightly higher torque values compared to the 2D model for most TSRs. This could indicate that the inclusion of three-dimensional effects in the modeling improves the accuracy of the predictions, albeit still falling short of the experimental results.

In terms of torque coefficient, the wind speed at 7 m/s, the rotor demonstrates high torque coefficients in both the 2D and 3D simulations across different TSRs, indicating efficient energy extraction from the wind. As the TSR increases, the torque coefficients decrease, which aligns with the expected behavior of Savonius rotors. Additionally, the 3D simulation consistently yields slightly higher torque coefficients compared to the 2D simulation, reflecting the added complexity captured in the three-dimensional simulation, such as flow separation and three-dimensional flow patterns. At a wind speed of 5 m/s, the torque coefficients for both simulations are lower than those at 7 m/s, indicating reduced energy extraction at the lower wind speed. Similarly, the torque coefficients decrease with increasing TSR, maintaining the expected trend for Savonius rotors. The 3D simulation continues to exhibit slightly higher torque coefficients, highlighting the advantages of considering three-dimensional flow effects for a more accurate representation of rotor performance. However, at a wind speed of 3 m/s, the torque coefficients further decrease, indicating diminished performance of the rotor at lower wind speeds. The trend of decreasing torque coefficients with increasing TSR persists, consistent with previous cases. Once again, the 3D simulation shows higher torque coefficients, emphasizing the significance of accounting for three-dimensional flow effects in the simulation. In summary, the simulation results illustrate that the two-bladed conventional Savonius rotor performs well at higher wind speeds, effectively extracting energy from the wind. However, its performance diminishes at lower wind speeds. The 3D simulation consistently exhibits higher torque coefficients, underscoring the importance of considering three-dimensional flow effects for a more accurate representation of rotor performance.

4.4 Comparison of Power Output and Torque Coefficient

Power represents the amount of energy generated by the rotor, while power coefficient allows us to compare the power output across different rotor designs and operating conditions. By comparing the power and power coefficient obtained from 2D and 3D simulations, the impact of three-dimensional effects on the rotor's power generation can be understood better. The results of the power output against TSR and power coefficient against TSR are plotted in Figure 6 and Figure 7, respectively. At a wind speed of 7 m/s, the power output of the rotor exhibits a positive correlation with the TSR. It is observed that at a TSR of 0.2, both the 2D and 3D simulations show relatively lower power values. However, as the TSR increases to 1.2, the power output substantially increases, indicating a more efficient energy extraction. This behavior aligns with the expected trend for Savonius rotors, as higher TSRs correspond to faster rotational speeds, leading to increased power generation. Comparing the 2D and 3D simulations, it can be observed that the 3D simulation consistently yields slightly higher power values across different TSRs. This suggests that the three-dimensional flow effects captured in the 3D simulation, such as flow separation and three-dimensional flow patterns, enhance the rotor's performance and improve power output compared to the simplified 2D simulation. Furthermore, at a wind speed of 5 m/s, the power output follows a similar trend as at 7 m/s. As the TSR increases, the power output increases as well. For instance, at a TSR of 0.2, the power values are relatively lower, but they progressively increase as the TSR reaches 1.2. This demonstrates the importance of higher rotational speeds for improved power generation. Consistently, the 3D simulation yields slightly higher power values compared to the 2D simulation, indicating the added benefits of considering three-dimensional flow effects in capturing more energy from the wind. At a wind speed of 3 m/s, the power output of the two-bladed conventional Savonius rotor follows a similar trend as in the higher wind speed cases. However, there are specific TSRs where a sudden drop in power occurs. For instance, at a TSR of 0.6, there is a significant decrease in power output compared to the neighboring TSRs. This drop can be attributed to the rotor operating in an unfavorable region of its performance curve. At this particular TSR, the rotor blades experience a combination of factors that negatively affect power generation.

One of the main factors is flow separation. As the rotor rotates at a higher speed, the flow around the concave side of the blades tends to separate, causing an inefficient transfer of momentum from the wind to the rotor. This flow separation results in reduced pressure differences between the blades, leading to a decrease in torque and subsequently in power output. Additionally, at certain TSRs, the interaction between the blades becomes unfavorable, leading to increased drag and reduced power generation. In the case of the sudden drop at a TSR of 0.6, it is possible that the interaction between the two blades at this specific rotational speed creates adverse flow patterns, causing higher drag forces and decreasing power output. Furthermore, it is worth noting that the aerodynamic characteristics of the Savonius rotor are influenced by the flow conditions, such as wind speed and blade geometry. At lower wind speeds like 3 m/s, the flow is relatively weaker, and the rotor may operate closer to stall conditions, where the flow separates more easily, resulting in reduced power output. In summary, the sudden drop in power at certain TSRs in the 3 m/s simulation can be attributed to a combination of factors, including flow separation, unfavorable blade interaction, and the rotor operating in less optimal flow conditions. These factors lead to decreased torque, reduced power output, and lower overall performance. Understanding these phenomena is crucial for optimizing the design and operational parameters of Savonius rotors to ensure efficient power generation across a range of wind speeds. Overall, it can be said that the simulation results highlight the influence of the TSR on the power output of the two-bladed conventional Savonius rotor. Higher TSRs, corresponding to higher rotational speeds, lead to increased power generation. The 3D simulation consistently shows slightly higher power values compared to the 2D simulation, indicating the importance of accounting for three-dimensional flow effects. These findings provide valuable insights for the design and optimization of conventional Savonius rotors, considering different wind speeds and TSRs to achieve higher power output and improved overall performance.

In terms of power coefficient, the relationship between the TSR and the power coefficients for both the 2D and 3D simulations is observed, as shown in Figure 7. As the TSR increases from 0.2 to

1.2, a gradual increase in the power coefficients for both the 2D and 3D simulations can be seen until a certain TSR where it begins to slowly decline. This means that the rotor becomes less efficient at converting wind energy into power as the TSR increases over a certain limit. However, it's important to note that even at higher TSRs, the power coefficients for the 3D simulation tend to be slightly higher compared to the 2D simulation. This suggests that the additional complexity and three-dimensional effects incorporated in the 3D simulation contribute to improved power generation capabilities. When the wind speed decreases to 5 m/s, similar trends in the power coefficients can be observed. As the TSR increases, the power coefficients increase for both the 2D and 3D simulations and then it drops slightly at some points. However, the overall power coefficients are lower at this wind speed compared to the data at 7m/s. This suggests that the rotor is less effective in harnessing wind energy and generating power at lower wind speeds. At a wind speed of 3m/s, we see a different behavior in the power coefficients compared to the higher wind speeds. Initially, as the TSR increases from 0.2 to 0.4, the power coefficients increase for both the 2D and 3D simulations. However, beyond a TSR of 0.4, the power coefficients suddenly drop for both simulations. This indicates that the rotor's performance is significantly influenced by the TSR at lower wind speeds. The sudden drop in power coefficients at higher TSRs for the 3m/s simulation suggests that there are certain operating conditions where the rotor experiences flow separation, stall, or increased drag. These factors can negatively affect the rotor's ability to efficiently capture wind energy and convert it into power. In summary, the data shows that the power coefficients for the 2D and 3D simulations of the two-bladed conventional Savonius rotor vary with the TSR and wind speed. The trends observed provide insights into the rotor's efficiency and performance characteristics under different operating conditions. This understanding can help in optimizing the rotor design and operating parameters to maximize power output in specific wind conditions.

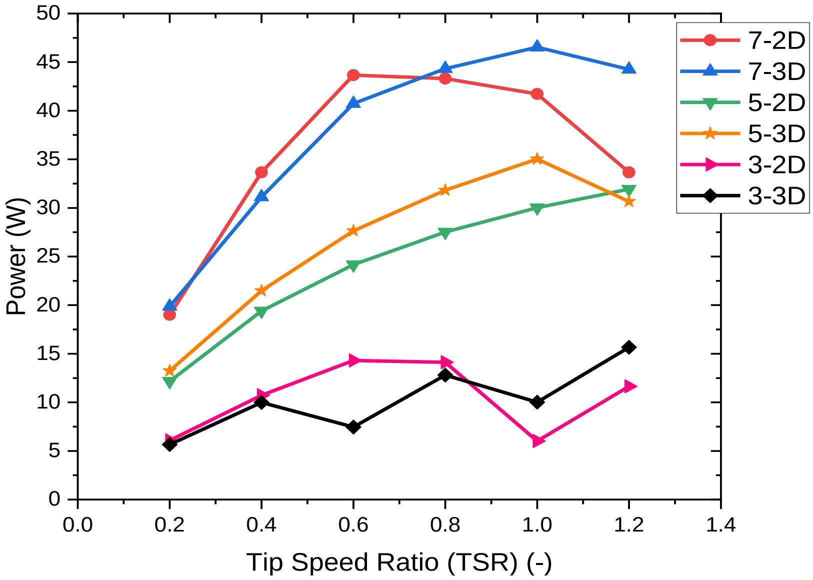

Fig. 6. Power output against TSR at different wind speeds

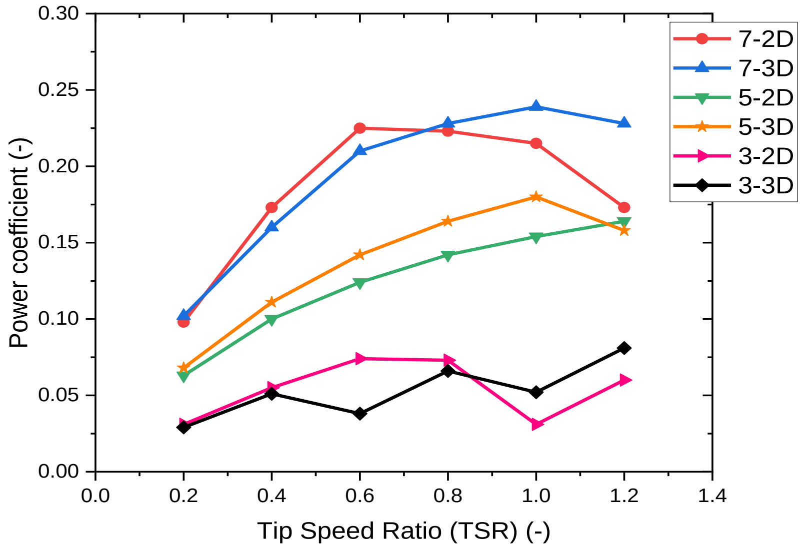

Fig. 7. Power coefficient against TSR at different wind speeds

4.5 Visualization and Flow Analysis

The visualization of velocity, pressure, streamline, and vector contour plays a crucial role in computational fluid dynamics (CFD) for several reasons, such as understanding flow patterns, identifying pressure distributions, validating simulations and many more. Figures 8, 9 and 10 show these four contours. The presence of returning blade wake vortices in the figure above refers to the formation of swirling flow structures behind the turbine blades. As the blades rotate and interact with the fluid, they create disturbances in the flow, resulting in the formation of vortices or swirls in the wake region downstream of the blades. The presence of forward and backward thrust indicates the generation of positive and negative axial forces on the turbine blades. This thrust is responsible for driving the turbine and extracting energy from the fluid flow. Contour plots representing the forward thrust show regions where the axial forces are predominantly directed in the forward or downstream direction. These contours usually exhibit higher values near the leading edge of the blades and decrease towards the trailing edge. Contour plots representing backward thrust depict regions where the axial forces are directed in the backward or upstream direction. These contours usually exhibit negative or low values near the leading edge and may increase towards the trailing edge. The pressure is lower downstream of the advancing and returning blades in Figure 10 due to flow separation. The upstream pressure is higher on the returning blade and peaks at the middle of the blade. Both turbine blades are subjected to drag force; the drag on the advancing blade drives the turbine, while the drag on the returning blade restricts it. Velocity contour plots in Figure 11 provide a visual representation of the flow field, illustrating the distribution of fluid velocities throughout the computational domain. In brief, the 2D analysis involves modeling the rotor as a two-dimensional object, with a cross-sectional area that varies with height. This simplifies the computational effort required to simulate the rotor and allows for faster analysis. However, 2D analysis neglects the effect of three-dimensional flow phenomena, such as tip vortices and end effects, which can significantly impact rotor performance. Therefore, 2D analysis may not accurately capture the complex flow dynamics that occur in a real-world Savonius rotor.

On the other hand, 3D analysis models the rotor as a three-dimensional object and takes into account the complex flow dynamics that occur in a real-world Savonius rotor. This results in a more accurate prediction of the rotor's performance, including the effects of tip vortices and end effects. However, 3D analysis requires significantly more computational resources than 2D analysis, which can make it prohibitively expensive for some applications. In summary, 2D analysis is faster and less computationally expensive than 3D analysis, but it may not capture the complex flow dynamics that occur in a real-world Savonius rotor. 3D analysis, on the other hand, provides a more accurate prediction of the rotor's performance but requires more computational resources. The choice between 2D and 3D analysis will depend on the specific application and the level of accuracy required.

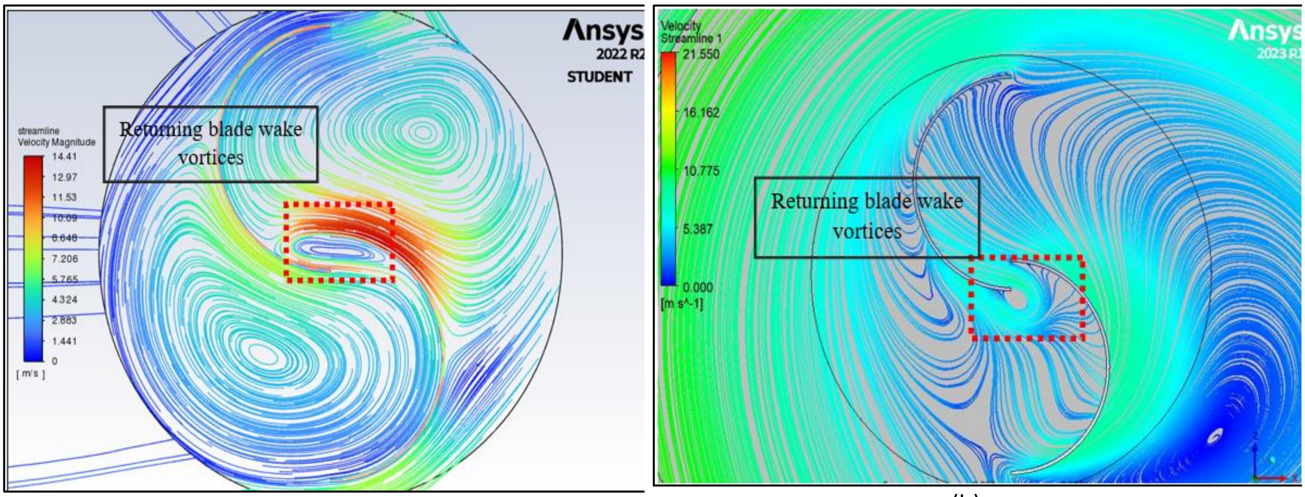

(a) (b)

Fig. 8. Velocity streamlines around the model (a) Velocity streamline for 2D simulation (b) Velocity streamline for 3D simulation

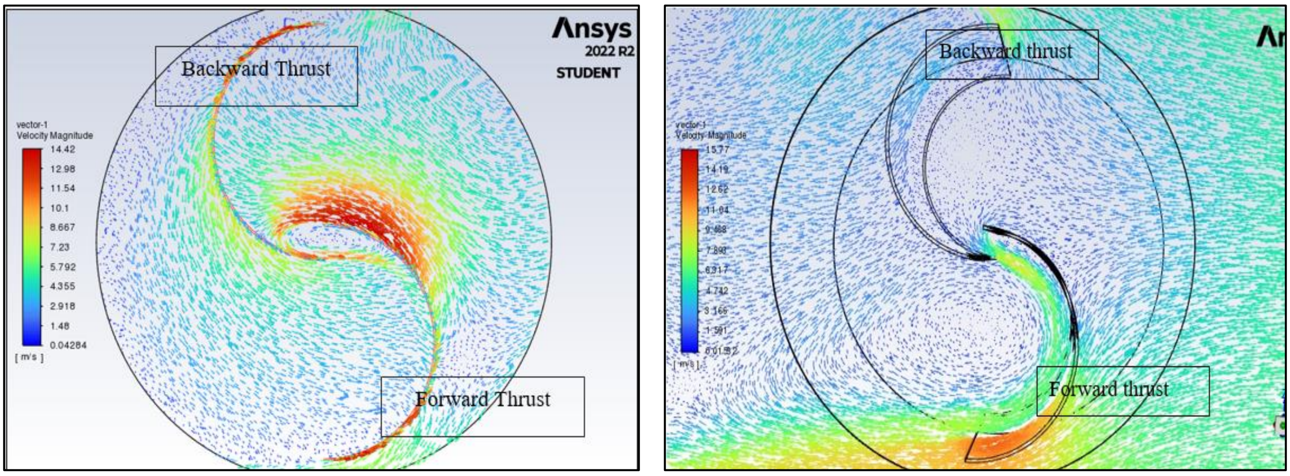

(a) (b)

Fig. 9. Velocity vector around the model (a) Vector contour for 2D simulation (b) Vector Contour for 3D simulation

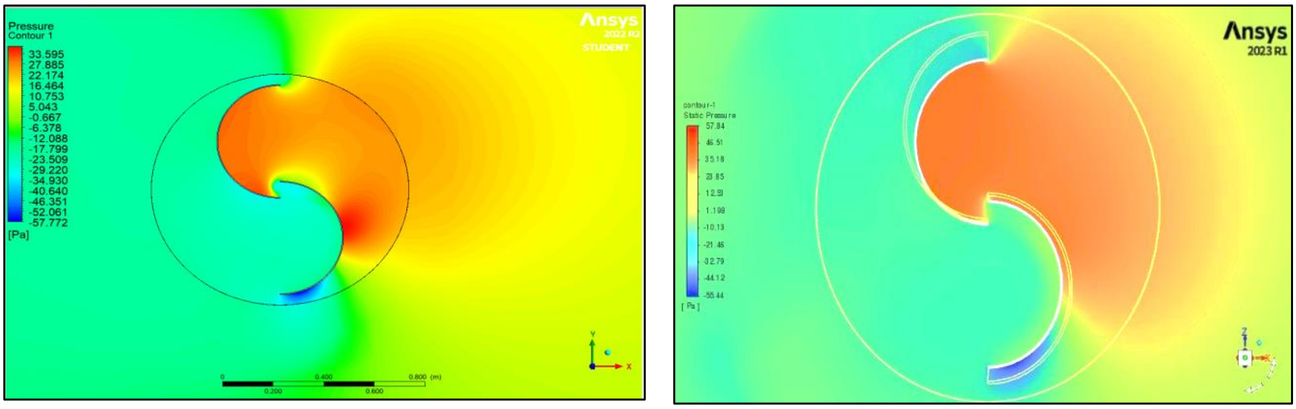

(a) (b)

Fig. 10. Pressure distributions around the model (a) Pressure contour for 2D simulation (b) Pressure contour for 3D simulation

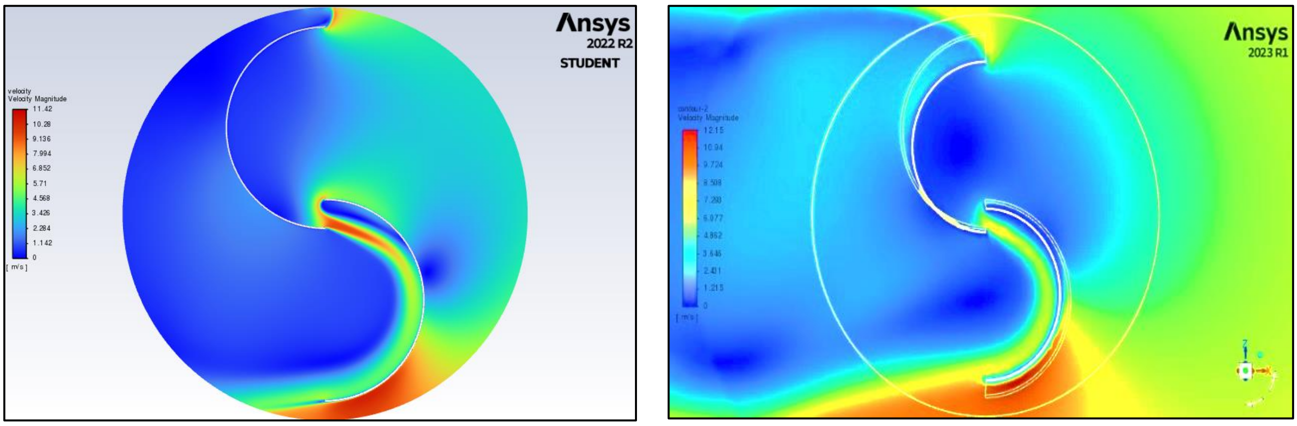

(a) (b)

Fig. 11. Velocity distributions around the model (a) Velocity Contour for 2D simulation (b) Velocity Contour for 3D simulation

5. Conclusions

In this investigation, the performance of the Savonius rotor was analyzed using both 2D and 3D analysis techniques. The 2D analysis is a simplified approach that assumes the flow behavior is two-dimensional and uniform, while the 3D analysis considers the three-dimensional and complex flow behavior around the rotor. The results of the investigation showed that the 3D analysis demonstrated better performance in terms of the coefficient of power (Cp) and torque coefficient (Ct) compared to the 2D analysis. The 3D analysis also showed a more accurate representation of the flow behavior around the rotor, including the wake effect and the boundary layer separation. However, the 2D analysis is still useful for initial design and feasibility studies due to its simplicity and computational efficiency. It can provide a quick estimation of the rotor performance and is suitable for parametric studies. On the other hand, the 3D analysis required more computational resources and time to simulate, but it provided a more detailed and accurate representation of the flow behavior around the rotor. Therefore, it is recommended to use both 2D and 3D analysis techniques in a complementary manner for a more comprehensive analysis of Savonius rotor performance. In conclusion, the investigation has demonstrated the importance of using both 2D and 3D analysis techniques for a comprehensive analysis of Savonius rotor performance. The results showed that the 3D analysis provides a more accurate representation of the flow behavior and better performance compared to the 2D analysis. However, the 2D analysis is still useful for initial design and feasibility studies due to its simplicity and computational efficiency. The findings of this investigation can be used to improve the design and performance of the Savonius rotor for urban wind energy applications.

Acknowledgement
Communication of this research is made possible through monetary assistance by Universiti Tun Hussein Onn Malaysia and the UTHM Publisher's Office via Publication Fund E15216.

References

[1] Xue, Chaokai, Muhammad Shahbaz, Zahoor Ahmed, Mahmood Ahmad, and Avik Sinha. "Clean energy consumption, economic growth, and environmental sustainability: what is the role of economic policy uncertainty?." *Renewable Energy* 184 (2022): 899-907. https://doi.org/10.1016/j.renene.2021.12.006
[2] Alquraishi, Balasem Abdulameer, Nor Zelawati Asmuin, Sofian Mohd, Wisam A. Abd Al-Wahid, and Akmal Nizam Mohammed. "Review on diffuser augmented wind turbine (dawt)." *International Journal of Integrated Engineering* 11, no. 1 (2019).
[3] Didane, Djamal Hissein, Abas Ab Wahab, S. Shamsudin, and N. Sand Rosly. "Wind as a sustainable alternative energy source in Malaysia-a review." *ARPN Journal of Engineering and Applied Sciences* 11, no. 10 (2016): 6442-6449.
[4] Mondal, Mithun, Djamal Hissein Didane, Alhadj Hisseine Issaka Ali, and Bukhari Manshoor. "Wind Energy Assessment as a Source of Power Generation in Bangladesh." *Journal of Advanced Research in Applied Sciences and Engineering Technology* 26, no. 3 (2022): 16-22. https://doi.org/10.37934/araset.26.3.1622
[5] Didane, Djamal Hissein, Abas Ab Wahab, Syariful Syafiq Shamsudin, Nurhayati Rosly, Mohd Fadhli Zulkafli, and Sofian Mohd. "Assessment of wind energy potential in the capital city of Chad, N'Djamena." In *AIP Conference Proceedings*, vol. 1831, no. 1. AIP Publishing, 2017. https://doi.org/10.1063/1.4981190
[6] Roga, Sukanta, Shawli Bardhan, Yogesh Kumar, and Sudhir K. Dubey. "Recent technology and challenges of wind energy generation: A review." *Sustainable Energy Technologies and Assessments* 52 (2022): 102239. https://doi.org/10.1016/j.seta.2022.102239
[7] Aktaş, Ahmet. "The importance of energy storage in solar and wind energy, hybrid renewable energy systems." In *Advances in Clean Energy Technologies*, pp. 377-403. Academic Press, 2021. https://doi.org/10.1016/B978-0-12-821221-9.00010-4
[8] Samsudin, Muhammad Zahid, Djamal Hissein Didane, Said A. Elshayeb, and Bukhari Manshoor. "Assessment of solar energy potential in johor, malaysia." *Journal of Design for Sustainable and Environment* 3, no. 1 (2021).
[9] Foteinis, Spyros. "Wave energy converters in low energy seas: Current state and opportunities." *Renewable and Sustainable Energy Reviews* 162 (2022): 112448. https://doi.org/10.1016/j.rser.2022.112448
[10] Mott, A., Alper Baba, M. Hadi Mosleh, Hatice Eser Ökten, Masoud Babaei, Ayşegül Yağmur Gören, Chao Feng et al. "Boron in geothermal energy: Sources, environmental impacts, and management in geothermal fluid." *Renewable and Sustainable Energy Reviews* 167 (2022): 112825. https://doi.org/10.1016/j.rser.2022.112825
[11] He, Lipeng, Yuhang Han, Renwen Liu, Renhui Hu, Gang Yu, and Guangming Cheng. "Design and performance study of a rotating piezoelectric wind energy harvesting device with wind turbine structure." *Energy* 256 (2022): 124675. https://doi.org/10.1016/j.energy.2022.124675
[12] Zhang, Jianhong, and Hao Wang. "Development of offshore wind power and foundation technology for offshore wind turbines in China." *Ocean Engineering* 266 (2022): 113256. https://doi.org/10.1016/j.oceaneng.2022.113256
[13] Hasankhani, Arezoo, Seyed Mehdi Hakimi, and Arash Vafaeizadeh. "Developing energy management system considering renewable energy systems in residential community." In *Design, Analysis, and Applications of Renewable Energy Systems*, pp. 275-299. Academic Press, 2021. https://doi.org/10.1016/B978-0-12-824555-2.00003-4
[14] Didane, D. H., Sofian Mohd, Z. Subari, Nurhayati Rosly, MF Abdul Ghafir, and MF Mohd Masrom. "An aerodynamic performance analysis of a perforated wind turbine blade." In *IOP Conference Series: Materials Science and Engineering*, vol. 160, no. 1, p. 012039. IOP Publishing, 2016. https://doi.org/10.1088/1757-899X/160/1/012039
[15] Loutun, Mark Jason Thomas, Djamal Hissein Didane, Mohd Faizal Mohideen Batcha, Kamil Abdullah, Mas Fawzi Mohd Ali, Akmal Nizam Mohammed, and Lukmon Owolabi Afolabi. "2D cfd simulation study on the performance of various naca airfoils." *CFD Letters* 13, no. 4 (2021): 38-50. https://doi.org/10.37934/cfdl.13.4.3850
[16] Dewan, Anupam, Adesh Gautam, and Rahul Goyal. "Savonius wind turbines: A review of recent advances in design and performance enhancements." *Materials Today: Proceedings* 47 (2021): 2976-2983. https://doi.org/10.1016/j.matpr.2021.05.205
[17] Al-Ghriybah, Mohanad, Mohd Fadhli Zulkafli, Djamal Hissein Didane, and Sofian Mohd. "Performance of the

savonius wind rotor with two inner blades at low tip speed ratio." *CFD Letters* 12, no. 3 (2020): 11-21. https://doi.org/10.37934/cfdl.12.3.1121
[18] Duc, Minh Banh, Hung Tran The, Khiem Pham Van, and Anh Dinh Le. "Predicting aerodynamic performance of savonius wind turbine: An application of generalized k-ω turbulence model." *Ocean Engineering* 286 (2023): 115690. https://doi.org/10.1016/j.oceaneng.2023.115690
[19] Halmy, Muhammad Syahmy Mohd, Djamal Hissein Didane, Lukmon Owolabi Afolabi, and Sami Al-Alimi. "Computational fluid dynamics (cfd) study on the effect of the number of blades on the performance of double-stage savonius rotor." *CFD Letters* 13, no. 4 (2021): 1-10. https://doi.org/10.37934/cfdl.13.4.110
[20] Didane, Djamal Hissein, Mohd Fadhli Zulkafli, Sofian Mohd, Mohd Faizal Mohideen Batcha, and Amir Khalid. "Development and performance investigation of a unique dual-rotor Savonius-type counter-rotating wind turbine." *International Journal of Integrated Engineering* 13, no. 6 (2021): 89-98.
[21] Akwa, Joao Vicente, Horacio Antonio Vielmo, and Adriane Prisco Petry. "A review on the performance of Savonius wind turbines." *Renewable and sustainable energy reviews* 16, no. 5 (2012): 3054-3064. https://doi.org/10.1016/j.rser.2012.02.056
[22] Maldar, Nauman Riyaz, Cheng Yee Ng, and Elif Oguz. "A review of the optimization studies for Savonius turbine considering hydrokinetic applications." *Energy Conversion and Management* 226 (2020): 113495. https://doi.org/10.1016/j.enconman.2020.113495
[23] K. A. H. Al-Gburi, F. B. I. Alnaimi, B. A. Al-quraishi, E. S. Tan, and M. M. Maseer, "A comparative study review: The performance of Savonius-type rotors," *Materials Today: Proceedings*, vol. 57, pp. 343–349, 2022. https://doi.org/10.1016/j.matpr.2021.09.226
[24] Dewan, Anupam, Ashok Kumar Bishnoi, Tej Pratap Singh, and Shivam Singh Tomar. "Elliptical Bladed Savonius Rotor for Wind Energy: Efficacy of RANS Modeling for Flow Characteristics." *Journal of Energy Resources Technology* 145, no. 5 (2023): 051301. https://doi.org/10.1115/1.4056275
[25] Tomar, Shivam Singh, Anupam Dewan, and Tej Pratap Singh. "Effects of axisymmetric-omnidirectional deflector on aerodynamics of modified Bach Savonius rotor for power enhancement." *Energy Conversion and Management* 297 (2023): 117720. https://doi.org/10.1016/j.enconman.2023.117720
[26] Montoya, Leidy Tatiana Contreras, Mohamed Yasser Hayyani, Mohamad Issa, Adrian Ilinca, Hussein Ibrahim, and Miloud Rezkallah. "Wind power plant planning and modeling." In *Hybrid renewable energy systems and microgrids*, pp. 259-312. Academic Press, 2021. https://doi.org/10.1016/B978-0-12-821724-5.00012-X
[27] Yuwono, Triyogi, Gunawan Sakti, Fatowil Nur Aulia, and Adi Chandra Wijaya. "Improving the performance of Savonius wind turbine by installation of a circular cylinder upstream of returning turbine blade." *Alexandria Engineering Journal* 59, no. 6 (2020): 4923-4932. https://doi.org/10.1016/j.aej.2020.09.009
[28] Banh Duc, Minh, Hung Tran the, Nguyen Dinh Duc, Trinh Chu Duc, and Anh Dinh Le. "Performance enhancement of savonius wind turbine by multicurve blade shape." *Energy Sources, Part A: Recovery, Utilization, and Environmental Effects* 45, no. 1 (2023): 1624-1642. https://doi.org/10.1080/15567036.2023.2180114
[29] Al-Ghriybah, Mohanad, Mohd F. Zulkafli, and Djamal H. Didane. "Numerical investigation of inner blade effects on the conventional savonius rotor with external overlap." *Journal of Sustainable Development of Energy, Water and Environment Systems* 8, no. 3 (2020): 561-576. https://doi.org/10.13044/j.sdewes.d7.0292
[30] Salleh, Mohd Badrul, Noorfazreena M. Kamaruddin, and Zulfaa Mohamed-Kassim. "The effects of deflector longitudinal position and height on the power performance of a conventional Savonius turbine." *Energy Conversion and Management* 226 (2020): 113584. https://doi.org/10.1016/j.enconman.2020.113584
[31] Didane, Djamal Hissein, Nurhayati Rosly, Mohd Fadhli Zulkafli, and Syariful Syafiq Shamsudin. "Numerical investigation of a novel contra-rotating vertical axis wind turbine." *Sustainable Energy Technologies and Assessments* 31 (2019): 43-53. https://doi.org/10.1016/j.seta.2018.11.006
[32] Didane, Djamal Hissein, Nurhayati Rosly, Mohd Fadhli Zulkafli, and Syariful Syafiq Shamsudin. "Performance evaluation of a novel vertical axis wind turbine with coaxial contra-rotating concept." *Renewable energy* 115 (2018): 353-361. https://doi.org/10.1016/j.renene.2017.08.070
[33] Didane, Djamal Hissein, Siti Masyafikah Maksud, Mohd Fadhli Zulkafli, Nurhayati Rosly, Syariful Syafiq Shamsudin, and Amir Khalid. "Performance investigation of a small Savonius-Darrius counter-rotating vertical-axis wind turbine." *International Journal of Energy Research* 44, no. 12 (2020): 9309-9316. https://doi.org/10.1002/er.4874
[34] Didane, D. H., S. M. Maksud, M. F. Zulkafli, N. Rosly, S. S. Shamsudin, and A. Khalid. "Experimental Study on the Performance of a Savonius-Darrius Counter-Rotating Vertical Axis Wind Turbine." In *IOP Conference Series: Earth and Environmental Science*, vol. 268, no. 1, p. 012060. IOP Publishing, 2019. https://doi.org/10.1088/1755-1315/268/1/012060
[35] Didane, Djamal Hissein, Muhammad Amir Zafran Saipul Anuar, Mohd Faizal Mohideen Batcha, Kamil Abdullah, Mas Fawzi Mohd Ali, and Akmal Nizam Mohammed. "Simulation study on the performance of a counter-rotating savonius vertical axis wind turbine." *CFD Letters* 12, no. 4 (2020): 1-11. https://doi.org/10.37934/cfdl.12.4.111

[36] Halmy, Muhammad Syahmy Mohd, Djamal Hissein Didane, Lukmon Owolabi Afolabi, and Sami Al-Alimi. "Computational fluid dynamics (cfd) study on the effect of the number of blades on the performance of double-stage savonius rotor." *CFD Letters* 13, no. 4 (2021): 1-10. https://doi.org/10.37934/cfdl.13.4.110

[37] Wenehenubun, Frederikus, Andy Saputra, and Hadi Sutanto. "An experimental study on the performance of Savonius wind turbines related with the number of blades." *Energy procedia* 68 (2015): 297-304. https://doi.org/10.1016/j.egypro.2015.03.259

[38] Thiyagaraj, J., I. Rahamathullah, G. Anbuchezhiyan, R. Barathiraja, and A. Ponshanmugakumar. "Influence of blade numbers, overlap ratio and modified blades on performance characteristics of the savonius hydro-kinetic turbine." *Materials Today: Proceedings* 46 (2021): 4047-4053. https://doi.org/10.1016/j.matpr.2021.02.568

[39] Chemengich, Sammy Jamar, Sadek Z. Kassab, and Eslam R. Lotfy. "Effect of the variations of the gap flow guides geometry on the savonius wind turbine performance: 2D and 3D studies." *Journal of Wind Engineering and Industrial Aerodynamics* 222 (2022): 104920. https://doi.org/10.1016/j.jweia.2022.104920

[40] Ferrari, G., D. Federici, Paolo Schito, Fabio Inzoli, and Riccardo Mereu. "CFD study of Savonius wind turbine: 3D model validation and parametric analysis." *Renewable energy* 105 (2017): 722-734. https://doi.org/10.1016/j.renene.2016.12.077

[41] Larin, Patrick, Marius Paraschivoiu, and Cevdet Aygun. "CFD based synergistic analysis of wind turbines for roof mounted integration." *Journal of Wind Engineering and Industrial Aerodynamics* 156 (2016): 1-13. https://doi.org/10.1016/j.jweia.2016.06.007

[42] Howell, Robert, Ning Qin, Jonathan Edwards, and Naveed Durrani. "Wind tunnel and numerical study of a small vertical axis wind turbine." *Renewable energy* 35, no. 2 (2010): 412-422. https://doi.org/10.1016/j.renene.2009.07.025